Separation Science and Technology
Publication details, including instructions for authors and subscription information:
http://www.informaworld.com/smpp/title~content=t713708471

Evaluation of Nickel Sulphide Prepared by Different Routes for Removal of ^{106}Ru from Alkaline Radioactive Liquid Waste

N. L. Sonar[a]; V. Pardeshi[a]; R. Shukla[b]; M. S. Sonavane[a]; T. P. Valsala[a]; Y. Kulkarni[a]; A. K. Tyagi[b]; C. P. Kaushik[c]; V. K. Manchanda[d]
[a] Waste Management Division, Bhabha Atomic Research Centre, Tarapur, India [b] Chemistry Division, Bhabha Atomic Research Centre, Trombay, India [c] Waste Management Division, Bhabha Atomic Research Centre, Trombay, India [d] Radiochemistry Division, Bhabha Atomic Research Centre, Trombay, India

Online publication date: 15 September 2010

To cite this Article Sonar, N. L. , Pardeshi, V. , Shukla, R. , Sonavane, M. S. , Valsala, T. P. , Kulkarni, Y. , Tyagi, A. K. , Kaushik, C. P. and Manchanda, V. K.(2010) 'Evaluation of Nickel Sulphide Prepared by Different Routes for Removal of ^{106}Ru from Alkaline Radioactive Liquid Waste', Separation Science and Technology, 45: 14, 2064 — 2075
To link to this Article: DOI: 10.1080/01496395.2010.504450
URL: http://dx.doi.org/10.1080/01496395.2010.504450

Separation Science and Technology, 45: 2064–2075, 2010

ISSN: 0149-6395 print/1520-5754 online
DOI: 10.1080/01496395.2010.504450

Taylor & Francis
Taylor & Francis Group

Evaluation of Nickel Sulphide Prepared by Different Routes for Removal of ^{106}Ru from Alkaline Radioactive Liquid Waste

N. L. Sonar,[1] V. Pardeshi,[1] R. Shukla,[2] M. S. Sonavane,[1] T. P. Valsala,[1] Y. Kulkarni,[1] A. K. Tyagi,[2] C. P. Kaushik,[3] and V. K. Manchanda[4]

[1]*Waste Management Division, Bhabha Atomic Research Centre, Tarapur, India*
[2]*Chemistry Division, Bhabha Atomic Research Centre, Trombay, India*
[3]*Waste Management Division, Bhabha Atomic Research Centre, Trombay, India*
[4]*Radiochemistry Division, Bhabha Atomic Research Centre, Trombay, India*

An attempt has been made to synthesize nickel sulphide (NiS) compound by different routes. The NiS material thus obtained was coated on polymethyl metha acrylate (PMMA) beads to form a composite material, which was subjected to its performance evaluation for uptake of ^{106}Ru from low level radioactive liquid waste (LLW) stream. Distribution Coefficient (K_d) of ^{106}Ru from LLW using NiS–PMMA composite beads was found to be in the range of 9000–12000 (ml/g). The effect of various parameters viz. pH, ionic strength, temperature, time equilibration, etc. towards the uptake of ^{106}Ru was investigated. The sorption mechanism was also studied. The ΔG, ΔH, and ΔS value for sorption were evaluated. The sorption was observed to be spontaneous and endothermic in nature. From the practical utilization point of view, the rate of uptake of ^{106}Ru by the composite material was studied. The data of sorption was investigated with Lagergren first-order, pseudo-first-order, and second-order plots. Its intraparticle diffusion mechanism was studied with the Weber Morris model. The kinetics was found to follow a pseudo-first-order pattern with intraparticle diffusion. However, intraparticle diffusion is not the rate controlling step.

Keywords Lagergren; low level radioactive liquid waste (LLW); nickel sulphide; polymethyl metha acrylate; ruthenium; sorption; Weber Morris

INTRODUCTION

Reprocessing of the spent fuel from the reactor generates broadly two categories of radioactive liquid waste stream, viz. high level liquid waste (HLW) and intermediate level radioactive liquid waste (ILW). The concentrate of the aqueous raffinate of the coextraction cycle in PUREX process is referred to as HLW. HLW in acidic conditions is stored in stainless steel tanks for its subsequent treatments, viz. actinide partitioning (1,2) or vitrification (3,4). The waste is concentrated prior to its vitrification. During the concentration process, nitric acid is recovered through a fractionator and subsequently the off-gases are condensed to collect the condensate stream. The condensates as well as the recovered acid are categorized as ILW. A major source of ILW, however, is the second cycle raffinate of PUREX process and is having activity in the range of mill curies per litre. All the streams are acidic in nature. These streams are neutralized by alkali, and this process introduces a large amount of salts in the waste. Major radionuclides present in these waste streams are ^{137}Cs, ^{90}Sr, ^{106}Ru, ^{125}Sb, and trace concentration of actinides. These neutralized waste streams are treated using a specific resorcinol formaldehyde–iminodiactetic acid (RF-IDA) ion exchange resin for ^{137}Cs and ^{90}Sr remediation.

However, prior to the ion exchange treatment, a major fraction of strontium and alpha radionuclides in ILW are removed by precipitation during the alkalification step which is an essential requirement of the ion exchange treatment process. The resultant supernatant solution contains ^{137}Cs and ^{106}Ru as major radionuclides. It is passed through RF resin column to specifically remove ^{137}Cs and residual ^{90}Sr from the waste (5). However, RF resin does not provide decontamination for ^{106}Ru and it quantitatively reports in the column effluent. Thus the radioactive effluent stream of ion exchange treatment process is referred to as low level waste (LLW). It comprises of ^{106}Ru and trace amount of ^{137}Cs, ^{90}Sr, and ^{125}Sb not held on the RF column. The conventional chemical treatment for the column effluent waste involves coprecipitation of ^{137}Cs with copper ferrocyanide and ^{90}Sr with barium sulphate. Ferric hydroxide precipitation is carried out as a flocculant, it also provides decontamination of ^{125}Sb. Coprecipitation of ^{106}Ru is conventionally carried out by

Received 1 October 2009; accepted 5 April 2010.
Address correspondence to N. L. Sonar, Waste Management Division, Bhabha Atomic Research Center, PO Ghivali, Tarapur, Maharashtra 401504, India. E-mail: aakash3010@rediffmail.com

$Fe(OH)_2$ precipitation which requires lots of pH adjustment and yields poor decontamination factor (DF) value. Thus there is a need to develop a treatment step which can yield high DF value for ^{106}Ru with the column effluent LLW stream.

In acidic waste stream Ru exist as a complex species of nitrosyl ruthenium like $RuNO(NO_3)_3(H_2O)_2$ and $RuNO(NO_3)_2(OH)(H_2O)_2$ etc. (6–9). With the number and type of ligand attached to the RuNO group, the complex can be cationic, neutral, or anionic. It may exist as ruthenate ion (RuO_4^{-2}) or perruthenate ion RuO_4^- in alkaline solution (11). However, Ru is also reported to exist as $RuNO(OH)_3 \cdot H_2O$ under alkaline condition (12).

A wide variety of methods are reported in the literature for the uptake of radioruthenium from various LLW streams which makes use of chemical coprecipitation methods (13–16), sorbents (13,17–23), extractants (23), and electro-oxidation (24). An earlier study of co-precipitation of Ru with NiS (25,26) gave good decontamination with respect to Ru. Concentration of 2500 ppm as Ni^{2+} and 1326 ppm as S^{2-} was found to be optimum to give a decontamination factor of about 60–250 for ^{106}Ru using multiple-step precipitation from a radioactive liquid waste containing high salt. However, the use of high concentration of chemicals for treatment of the waste generates a large volume of sludge. In order to minimize the secondary waste in the form of sludge, efforts were made to convert the NiS into a spherical bead form by adsorbing it on a suitable substrate so as to use it effectively in the column mode operation (27). Synthesis of NiS by different methods such as conventional precipitation, polyol method (28,29) is well reported.

In the present work, NiS was prepared by various routes and a composite material was made by using NiS powder and Polymethyl metha acrylate (PMMA) beads. The composite material was evaluated for ^{106}Ru uptake. The sorption behavior was evaluated with the help of different sorption isotherms and the thermodynamic parameters were also evaluated. The rate of uptake of ^{106}Ru on the composite material was investigated with the Lagergren plot pattern of first-order, pseudo-first-order, and second-order. The Weber Morris model was applied to understand the intraparticle diffusion mechanism for sorption of ^{106}Ru on composite material.

EXPERIMENTAL

All reagents used in this study were of AR grade.

Synthesis of Nickel Sulphide

In the polyol method, the stoichiometric amount of nickel nitrate and thiourea were placed in a 500 ml round bottomed flask. The flask was filled with 150 ml of glycerol/ethylene glycol solution and stirred for a few minutes. The solution was refluxed at 140–150°C for 3 hours. Thereafter, the contents of the flask were filtered and washed several times with absolute alcohol and distilled water to remove unreacted chemicals. The solid product obtained was dried in air at 60°C. The NiS powder thus obtained was characterized by powder X-ray difractometer (XRD) and Energy Dispersive X-ray Analysis (EDX).

Preparation of NiS–PMMA Composite Beads

The NiS–PMMA composite material was prepared by coating the NiS powder on the surface of Polymethyl Methacrylate beads using suitable solvent as adhesive. Uniform coating of NiS powder on PMMA beads was achieved by making thick paste of NiS powder (140 ASTM mesh −100 micron) with methyl methacrylate monomer as adhesive and dispersing the paste over the PMMA beads of 0.5–0.6 mm diameter size. These composite beads were finally dried at 50°C in oven. The NiS–PMMA composite beads with NiS content varying from 1%–50% (wt/wt) were prepared by mixing the NiS powder.

The NiS-PMMA composite beads prepared were termed as

(i) NiS–PMMA conventional NiS powder – NiS–PMMA (C)
(ii) NIS–PMMA Polyol (Glycerol) NiS powder – NiS–PMMA(G) and
(iii) NiS–PMMA Polyol (ethylene glycol) NiS powder – NiS–PMMA(E).

For all experimental study, 10% composite material was used.

Preparation of Synthetic Low Level Waste (SLLW)

As discussed in the Introduction section of this paper, the actual radioactive condensate waste obtained from vitrification operation is acidic in nature. During the ion exchange treatment process the waste is made alkaline and then passed through RF resin column. However, for the present work, ^{137}Cs from acidic waste was removed by treatment with ammonium molybdenum phosphate (AMP) based composite material (30) and the resultant solution was made alkaline and taken up for further experimental study. The properties of the waste are listed in Table 1.

TABLE 1
Properties of the synthetic alkaline radioactive liquid waste

Sr. No.	Properties	Value
1	PH	11.0
2	Total solids, % (wt/vol)	3.0
3	Gross beta, mCi/L	2.0
5	^{137}Cs, mCi/L	2.7×10^{-4}
6	^{106}Ru, mCi/L	3.13×10^{-3}
7	^{125}Sb, mCi/L	5.81×10^{-3}

EVALUATION OF NIS – PMMA COMPOSITE MATERIAL

Distribution Coefficient (K_d) Value

0.1 g of the sorbent material prepared above was equilibrated with 10 ml of SLLW for one hour. The initial and final activity of ^{106}Ru was monitored using HPGe 8 K multichannel analyzer. The K_d value was calculated as follows.

$$K_d = \frac{C_i - C_f}{C_f} \times \frac{V}{W} \quad (ml/gm) \tag{1}$$

where C_i and C_f are the initial and final radioactivity content of ^{106}Ru (mCi/L), V is the volume (ml) of waste, and W is weight(g) of the composite material.

The effect of various parameters like pH, NiS–PMMA composition and ionic concentration on K_d value was studied.

Sorption Study

0.1 g of the sorbent material was equilibrated with 10 ml of inactive ruthenium solution containing ^{106}Ru as tracer at pH 11.0. The concentration of ruthenium was varied from 9.9×10^{-3} mmol/L to 4.95×10^{-2} mmol/L to understand the sorption behavior. The amount of adsorbed Ru was subjected to various adsorption isotherms like Langmuir, Dubinin–Radushkevich, and Freundlich isotherms to understand the sorption behavior.

Kinetic Experiments

To optimize the time for maximum uptake of Ru by the NiS–PMMA composite material, the composite material was equilibrated with SLLW for different time interval. The percentage uptake with respect to the time period was calculated using the following equation.

$$\%\ uptake = \frac{C_i - C_f}{C_f} \times 100 \tag{2}$$

where C_i and C_f are the initial and final concentrations of ^{106}Ru (mCi/L).

RESULT AND DISCUSSION

Polyol Method for Synthesis of NiS

During the experiment, the glycol or glycerin helps to provide a medium with a uniform reaction temperature and makes the reactants mix uniformly, which is important for the formation of the homogeneously distributed nanoscale crystallites. Nickel nitrate on mixing with thiourea in glycol or glycerin medium forms Ni(II) – thiourea complexes (31–33). The formation of metal sulfides product occurs due to the thermal decomposition of metal – thiourea complex.

Physical Characterisation

XRD of the samples showed a broad hump which may be due to the amorphous nature of the compounds. EDX analysis revealed the ratio of Ni to S as almost 1:1. The zeta potential measurement revealed the positive value at higher pH which was required for sorption of polyanionic species of ^{106}Ru. The surface area of the samples were evaluated by BET technique and were found to be 34.12, 28.83, and 29.17 m^2/g for conventional, glycerol, and ethylene glycol synthesized powders respectively.

Distribution Coefficient (K_d) Value

The K_d value was found to be 15000 and 26000 for the conventional and polyol NiS powder with the SLLW, respectively. It was evident that the ^{106}Ru peak almost disappeared after equilibration. Both the composite materials were found to be performing satisfactorily in alkaline conditions (Fig. 1). In acidic condition the lower K_d value can be explained due to the dissolution of NiS in acidic media.

As seen from Fig. 2, the K_d value is varying from 4200–9000 for the NiS–PMMA(C) composite material having NiS content varying from 10%–50% and it is from 250–13300 for the NiS–PMMA(G) material having NiS content varying from 1%–50%. In case of NiS–PMMA(C) the Kd value gradually increased and got stabilized at about 30% of NiS whereas it got stabilized at about 20% NiS content in case of NiS–PMMA(G). Further increase in NiS content, resulted in marginal increase in K_d value. This indicates that above 30 wt% of NiS in NiS–PMMA(C) and above 20 wt% in case of NiS–PMMA(G) material, there may be a formation of a multilayer over the PMMA beads or excess NiS powder may not be a getting coated over PMMA beads. However, during preparation of the NiS–PMMA composite material, no powder was left

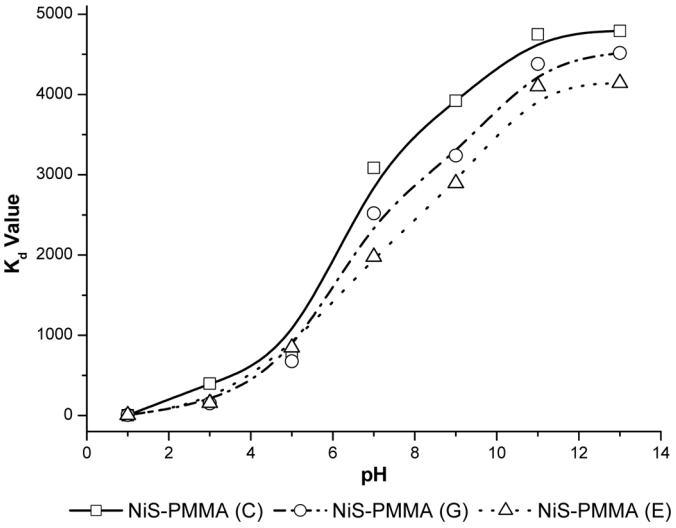

FIG. 1. Effect of pH on K_d value (10% composite material).

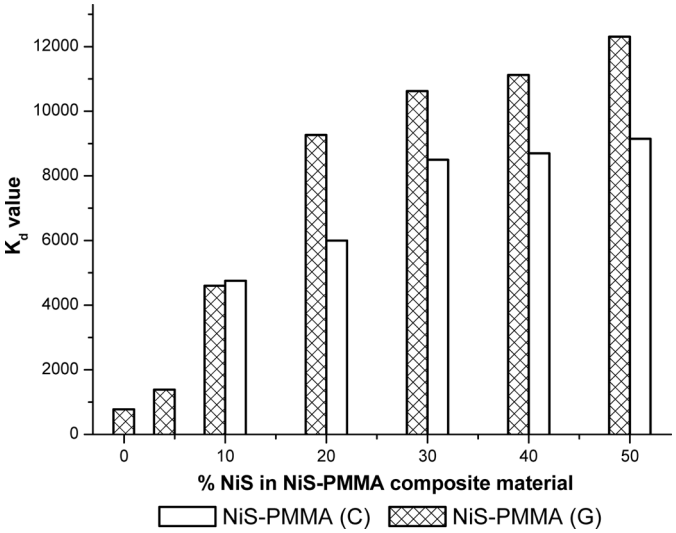

FIG. 2. Effect of %NiS content in the composite material on K_d value (pH 11.0).

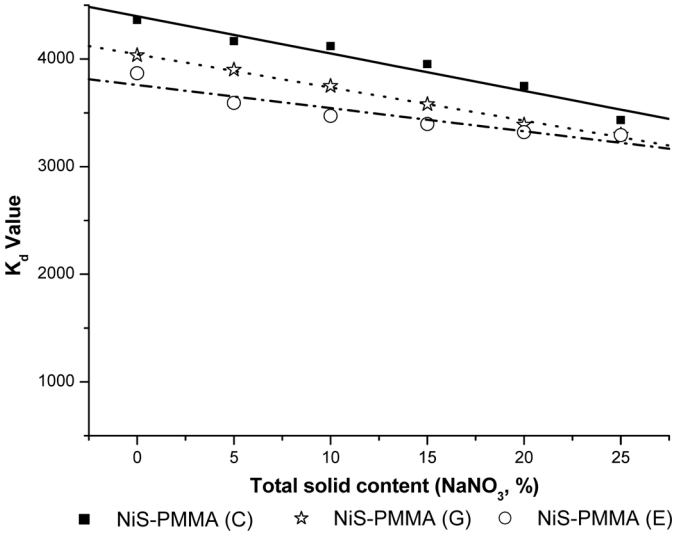

FIG. 4. Effect of salt concentration on Kd value (pH 11.0).

behind indicating a multilayer formation over the PMMA beads. This shows that the particle size in case of polyol NiS is smaller than that of conventional NiS.

From the kinetic study (Fig. 3), it is observed that the equilibrium condition has been achieved within 25 minutes indicating fast sorption kinetics.

During neutralization of the acidic waste streams, lots of salt in the form of sodium nitrate form in the waste solution which may affect during the treatment process. In view of this, variation of K_d with salt content was studied and it was found that there is not much effect of salt concentration on K_d value (Fig. 4). With an increase in salt concentration, the K_d value is decreasing marginally.

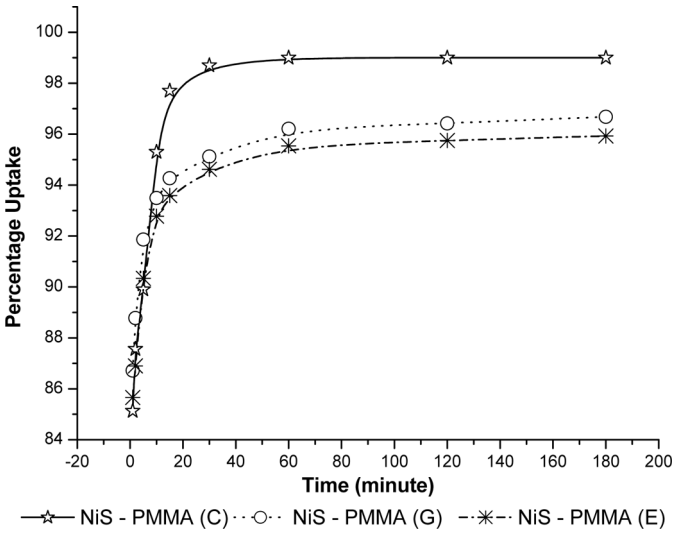

FIG. 3. Uptake of ^{106}Ru with respect to time.

Adsorption Isotherms

The sorption studies of ^{106}Ru on NiS–PMMA composite material were conducted and the sorption data were evaluated for different types of isotherms such as Langmuir, Freundlich, and Dubenin–Rodushkevich (D-R) isotherms.

Langmuir Adsorption Isotherm

The Langmuir isotherm model has been successfully applied to many adsorption processes and it is the most common model for the adsorption of solute from a liquid solution. Though the Langmuir adsorption isotherm was developed originally for the sorption of gases on the solid surface, it is also applied for the liquid–solid phases. The Langmuir adsorption isotherm in the liquid phase can be represented by the equation (34)

$$\frac{C_e}{q_e} = \frac{1}{q_o b} + \frac{C_e}{q_o} \tag{3}$$

where C_e is the equilibrium concentration of metal ions in the aqueous phase, q_e is the amount of metal ions sorbed on the solid phase at equilibrium, and q_o and b are the Langmuir constant related to the sorption capacity of the metal ions and energy of adsorption respectively. The graph is obtained when C_e/q_e was plotted against C_e over the concentration range of Ru investigated (Fig. 5).

Dubinin–Radushkevich (D–R) Isotherm

D–R isotherm (35) is significant within an adsorption "space" close to the sorbent surface. If the surface is heterogeneous and an approximation to a Langmuir isotherm is chosen as a local isotherm for all sites that are energetically equivalent, then the quantity $\beta^{1/2}$ can be related to the

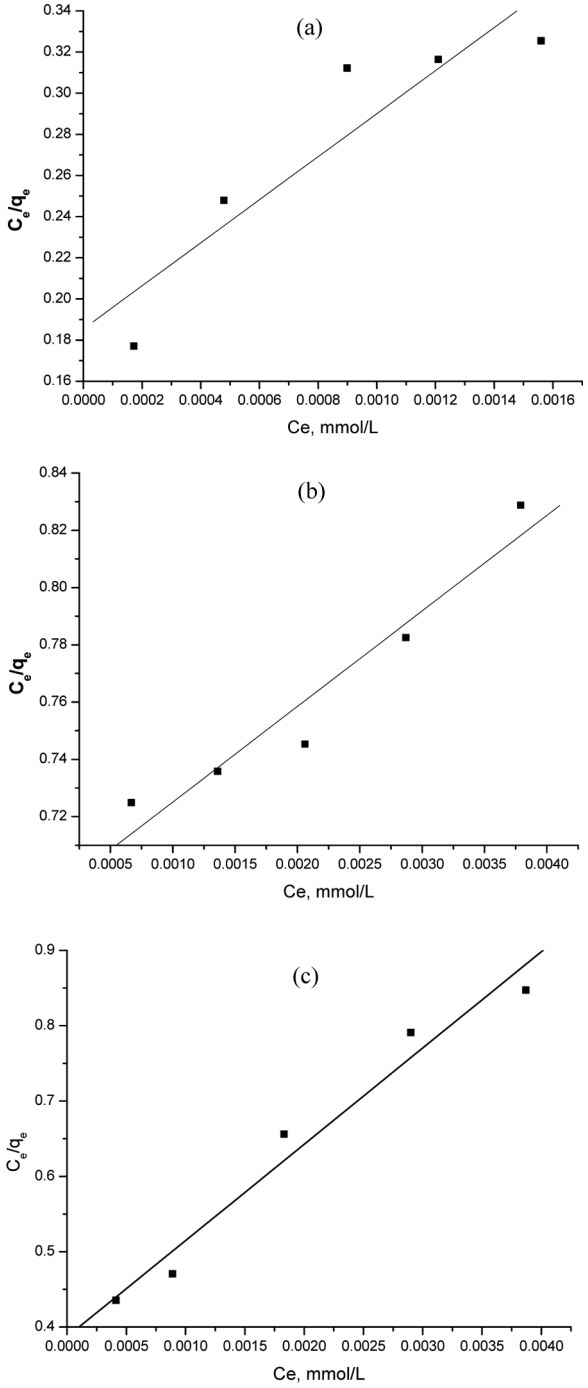

FIG. 5. Langmuir sorption isotherm; (a) NiS–PMMA(C); (b) NiS–PMMA(G); (c) NiS–PMMA(E).

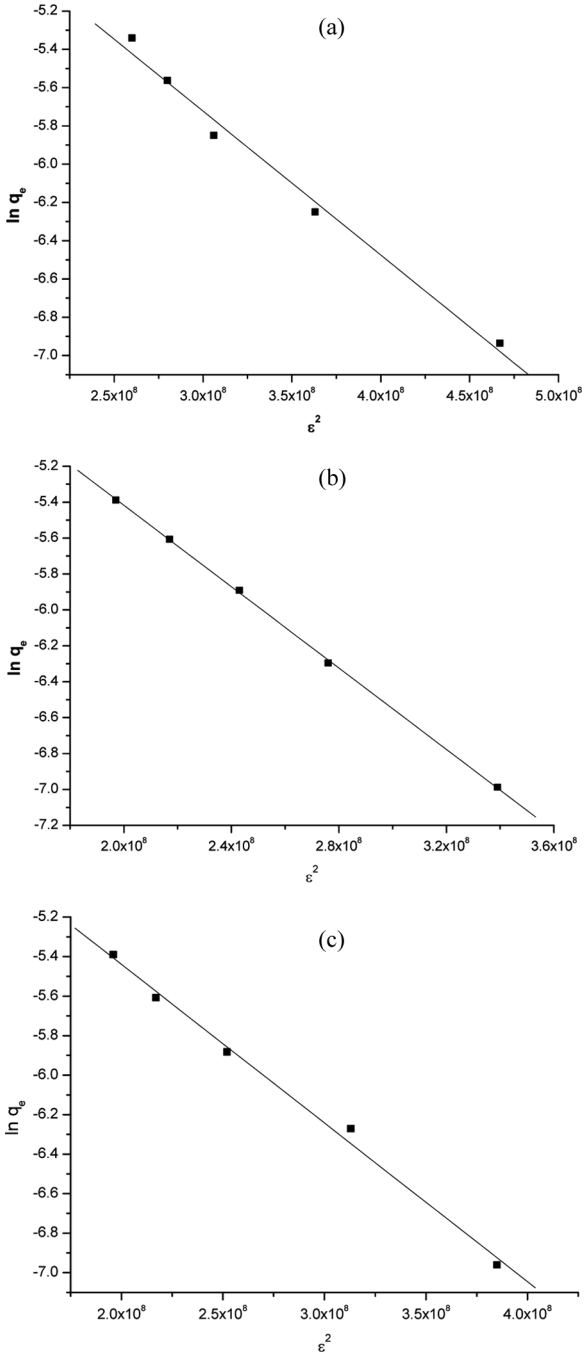

FIG. 6. D–R sorption isotherm; (a) NiS–PMMA(C); (b) NiS–PMMA(G); (c) NiS–PMMA(E).

mean sorption energy, E which is the free energy of the transfer of ruthenium from infinity to the surface of the sorbent. The difference in the free energy between the adsorbed phase and saturated liquid sorbate is referred to as adsorption potential which was first put forward by Polanyi (36) and later developed by Dubenin and his coworkers. The linearized form of the D-R isotherm is given by following equation.

$$\ln q_e = \ln X_m - \beta\varepsilon^2 \quad (4)$$

where Xm is the maximum sorption capacity β is the activity coefficient related to mean sorption energy, and ε

TABLE 2
Adsorption isotherm parameters

	D–R isotherm	Freundlich isotherm
NiS–PMMA(C)	$\beta = -7.52 \times 10^{-9}\,\mathrm{mol^2 \cdot KJ^{-2}}$; $\mathrm{E} = 8.153\,\mathrm{KJ \cdot mol^{-1}}$; $\mathrm{X_m} = 0.0312\,\mathrm{mmol \cdot g^{-1}}$	$1/\mathrm{n} = 0.7119$; $\mathrm{K_f} = 0.454\,\mathrm{mmol \cdot g^{-1}}$
NiS–PMMA(G)	$\beta = -1.13 \times 10^{-8}\,\mathrm{mol^2 \cdot KJ^{-2}}$; $\mathrm{E} = 6.651\,\mathrm{KJ \cdot mol^{-1}}$; $\mathrm{X_m} = 0.0428\,\mathrm{mmol \cdot g^{-1}}$	$1/\mathrm{n} = 0.929$; $\mathrm{K_f} = 0.838\,\mathrm{mmol \cdot g^{-1}}$
NiS–PMMA(E)	$\beta = -1.13 \times 10^{-8}\,\mathrm{mol^2 \cdot KJ^{-2}}$; $\mathrm{E} = 7.891\,\mathrm{KJ \cdot mol^{-1}}$; $\mathrm{X_m} = 0.0216\,\mathrm{mmol \cdot g^{-1}}$	$1/\mathrm{n} = 0.677$; $\mathrm{K_f} = 0.198\,\mathrm{mmol \cdot g^{-1}}$

Polanyi potential is given by the equation.

$$\varepsilon = RT \ln\left(1 + \frac{1}{C_e}\right) \tag{5}$$

where R is the gas constant in $\mathrm{kJ \cdot mole^{-1}}$ and T is the temperature in Kelvin.

The saturation limit (X_m) may represent the total specific micropore volume of the sorbent. The sorption space in the vicinity of a solid surface is characterized by a series of equipotential surfaces having the same sorption potential. This sorption potential is independent of temperature but varies according to the nature of sorbent and sorbate. The plot of ln q_e versus ε^2 as shown in Fig. 6 is a straight line. From the slope and the intercept values of the plot, the values of β and of X_m have been estimated as given in Table 2. The mean sorption energy (E) is the free energy change when one mole of the ion is transferred to the surface of the solid from infinity in solution (37) and can be calculated by using the following relationship.

$$E = \frac{1}{\sqrt{-2\beta}} \tag{6}$$

Freundlich Sorption Isotherm

The sorption data were also tested on the following linearized form of the Freundlich sorption isotherm.

$$\log\left(\frac{x}{m}\right) = \log K_f + \frac{1}{n}\log C_e \tag{7}$$

A linear plot is obtained when log(x/m) was plotted against log C_e over the concentration range investigated (Fig. 7). From the slope and intercept of the straight portion of the plot the values of Freundlich parameter, i.e., 1/n and K_f are computed and given in Table 2. These values signify the sorption intensity and capacity. The correlation factor computed for the linear regression analysis came out to be close to unity. The Freundlich sorption isotherm, one of the most widely used mathematical descriptions, usually fits the experimental data over a wide range of concentration.

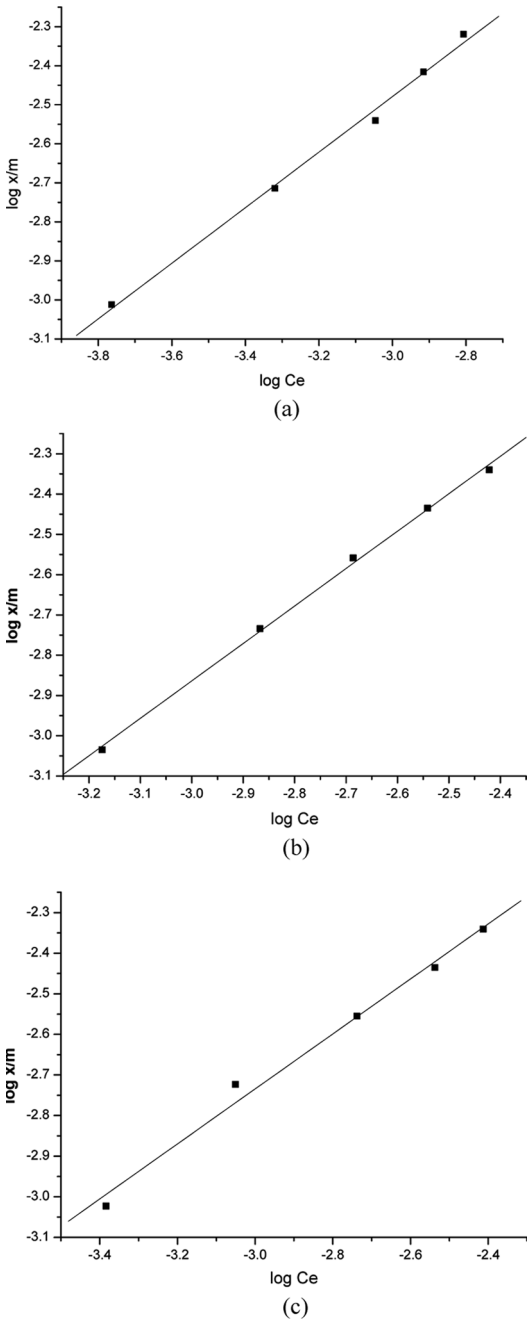

FIG. 7. Freundlich sorption isotherm; (a) NiS–PMMA(C) (b) NiS–PMMA(G) (c) NiS–PMMA(E).

It can be seen from all the data that the value of 1/n for Freundlich sorption isotherm is less than unity. This has physicochemical significance with reference to the qualitative characteristics of the isotherms as well as to the interaction of metal ion species and sorbent surface. It also indicates an increase in tendency for sorption with increasing solid phase concentration.

Although the Freundlich and Langmuir constants K_f and q_0 have different meanings, they led to the same conclusion about the correlation of the experimental data with the sorption model. The basic difference between K_f and q_0 is that the Langmuir isotherm assumes adsorption free energy independent of both the surface coverage and the formation of monolayer and the solid surface reaches saturation, while the Freundlich isotherm does not predict saturation of the solid surface by the adsorbate and therefore the surface coverage being mathematically unlimited. In conclusion, q_0 is the monolayer sorption capacity while K_f is the relative adsorption capacity or sorption power.

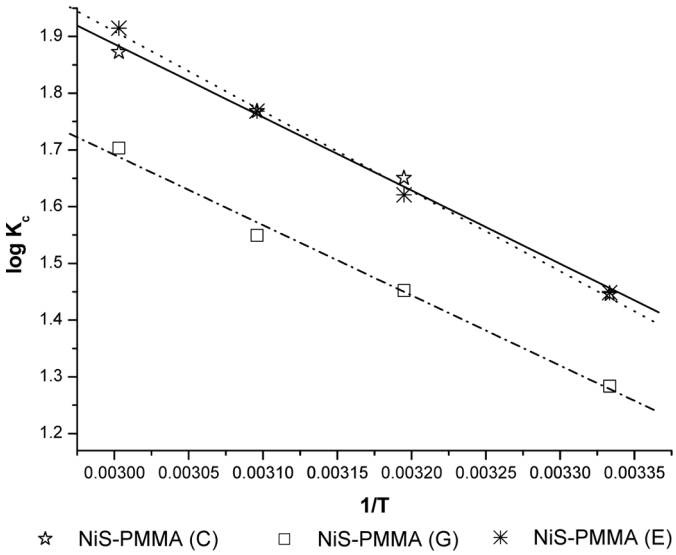

FIG. 8. Influence of temperature on sorption behavior of ^{106}Ru.

THERMODYNAMIC STUDIES

According to the adsorption theory, adsorption decreases with increase in temperature. However, at a higher temperature, increasing molecular motion and decreasing the viscosity of the solution leading to increase in adsorption has also been reported in case of activated carbon (38).

The influence of temperature variation was examined on the sorption of ruthenium at temperature 25, 40, 50, and 60°C. The plot of log K_c versus 1/T is shown in Fig. 8. The value of K_c, the equilibrium constant, can be worked at each temperature using the following relationship,

$$K_c = \frac{F_e}{1 - F_e} \tag{8}$$

where, F_e is the fraction sorbed at equilibrium and is given by

$$F_e = \frac{A_i - F_i}{A_i} \tag{9}$$

where *Ai* and *Fi* are initial and final concentration of the adsorbing species.

The equations given below may be used to evaluate the values of ΔG, ΔH, and ΔS.

$$\Delta G = -RT \ln K_c$$
$$\Delta G = \Delta H - T\Delta S$$
$$-2.303\ RT \log K_c = \Delta H - T\Delta S \tag{10}$$

$$\log K_c = \frac{-\Delta H}{2.303RT} + \frac{\Delta S}{2.303R} \tag{11}$$

From the slope and intercept of the plot between logK_c versus 1/T in Fig. 7, the values ΔH and ΔS were computed and from Eq. (11) ΔG, are computed as given in Table 3. The adsorption of metal ions increases with increasing temperature, which indicates the strengthening of the adsorbate–adsorbent interaction at high temperature. The increase in adsorption with temperature suggested that the active surface centers for sorption increase with temperature. Another reason may be due to the change in pore size and enhanced rate of intraparticle diffusion of solute as diffusion is an endothermic process. It is evident from Table 3 that the value of ΔG is negative

TABLE 3
Thermodynamic parameters

	Temperature (K)	ΔG (kJ/mmol)	ΔH (kJ/mmol)	ΔS (J/mol · K)
NiS–PMMA(C)	300	−8.305	10.731	110.25
	313	−9.891		
	323	−10.936		
	333	−11.939		
NiS–PMMA(G)	300	−6.834	23.77	100.17
	313	−8.379		
	323	−9.346		
	333	−10.191		
NiS–PMMA(E)	300	−8.320	26.99	117.50
	313	−9.715		
	323	−10.936		
	333	−12.207		

indicating spontaneous nature of sorption. The value of ΔH is positive indicating the endothermic nature of sorption. The possible explanation is that in order to adsorb the ions, they are to some extent dehydrated, which requires energy (39). The dehydration of hydrated ion is essentially an endothermic process and it appears that the endothermicity of the desolvation process exceeds the heat of adsorption. The lowering in the ΔG value with increasing temperature shows that adsorption of ions on NiS–PMMA composite material surface becomes favorable at high temperature. Since the adsorption is endothermic, the adsorption process is therefore made spontaneous because of positive entropy changes.

The sorption mechanism was studied with the Weber Morris model. The data of sorption was subjected to various kinetic models like Lagergren first-order, pseudo-first-order, and second-order plots.

Weber–Morris Intra Particle Diffusion Model

Adsorption kinetics is usually controlled by diffusion mechanisms, including the rapid external or boundary layer diffusion which causes surface adsorption, a gradual adsorption stage due to intraparticle diffusion, and plateau to equilibrium (40). A graphical method was introduced by Weber and Morris to prove the occurrence of intraparticle diffusion and to determine if it was a rate-determining step (41). According to this model the intraparticle diffusion is characterized by the equation

$$q_t = K_{id} t^{1/2} + I \tag{12}$$

where,

q_t = amount adsorbed at time t ($\mu \cdot \mathrm{Ci} \cdot \mathrm{g}^{-1}$)
K_{id} = the intra particle diffusion rate constant ($\mu \cdot \mathrm{Ci} \cdot \mathrm{g}^{-1} \cdot \mathrm{min}^{-1/2}$)
I = a constant value, which gives an idea about the thickness of the boundary layer, i.e., the larger the value the greater is the boundary layer effect (42).

If the intraparticle diffusion mechanism is involved then a plot of q_t versus $t^{1/2}$ will give a straight line and the line will pass through the origin if the intraparticle diffusion would be the rate-determining step (43).

To see whether the sorption kinetics of ^{106}Ru on the NiS–PMMA composite material is having intraparticle diffusion mechanism, a plot of q_t versus $t^{1/2}$ is drawn as given in Fig. 9

The linearity of the plot suggests that an intraparticle diffusion mechanism is involved. Since the straight line does not pass through the origin, the intraparticle diffusion is not the rate-determining step (44).

The intraparticle diffusion rate constant (K) and the value of I for the three composite materials is given below in Table 4.

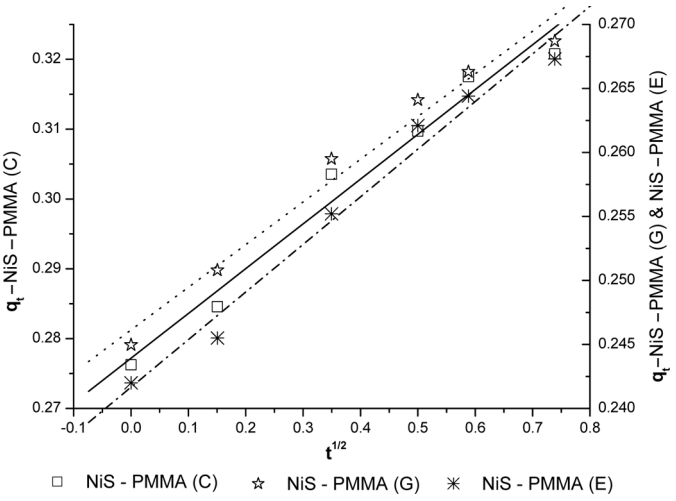

FIG. 9. Weber–Morris plot for ^{106}Ru sorption on NiS–PMMA composite material.

Sorption Kinetics

The phase adsorption kinetics in terms of the fractional attainment of equilibrium is expressed by the equation (45)

$$F = \frac{[M^R]_t}{[M^R]_{eq}} \tag{13}$$

where $[M^R]_t$ and $[M^R]_{eq}$ are the concentration of ^{106}Ru on solid phase at time 't' and at equilibrium respectively.

Figure 10 shows the plot of (1 – F) versus time 't'. The uptake of ruthenium is fast in the initial stages of the contact period and thereafter, it becomes slower near equilibrium. It is evident from the plot that more than 90% sorption was reached in about 15 minutes. The high initial rate has resulted due to the availability of a large number of vacant surface sites for adsorption.

Kinetic Models

The kinetic studies of a sorption process are paramount because the data obtained from such studies are necessary to understand the variables that influence the sorption. The results can also be used to determine the equilibrium time and rate of adsorption which in turn can be used to develop predictive models for column experiments. In order to define the sorption kinetics of ^{106}Ru on the NiS–PMMA composite

TABLE 4
Weber Morris plot constants

Material	K_{id}	I	R
NiS–PMMA(C)	0.0641	0.277	0.9866
NiS–PMMA(G)	0.0333	0.246	0.9872
NiS–PMMA(E)	0.0372	0.2416	0.9898

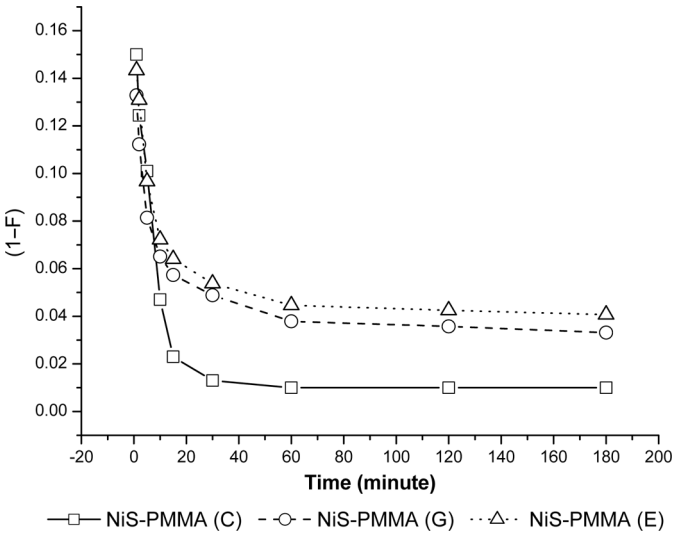

FIG. 10. Kinetics for sorption of Ru on the NiS–PMMA composite material.

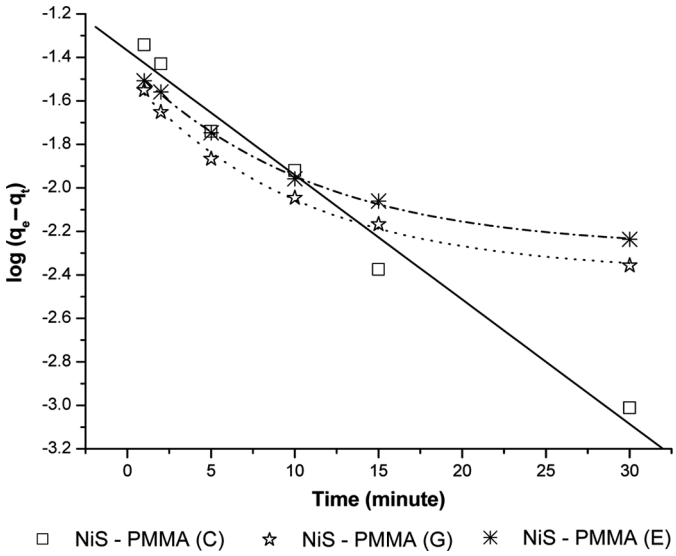

FIG. 11. Lagergren first order plot for Ru sorption on NiS–PMMA composite material.

materials, Langergren first-order, pseudo-second-order, and second-order kinetic models were studied.

(i) *Langergren first-order kinetics model*
For a batch contact time process, where the rate of sorption of Ru on the sorbent is proportional to the amount of Ru sorbed from solution, the first-order Langergren kinetics equation may be expressed as (46,47)

$$\log(q_e - q_t) = \log q_e - \frac{K_L}{2.303} t \tag{14}$$

where q_e and q_t are the amount of Ru sorbed at equilibrium and at time t respectively and K_L is the rate constant for first-order sorption (min^{-1}).

A first-order plot of $\log(q_e - q_t)$ versus t for sorption of Ru on the NiS–PMMA composite material is given in Fig. 11. The kinetic constants for the first-order model are given in Table 5.

(ii) *Pseudo second-order model*
To describe the sorption, a modified pseudo-second-order equation is expressed as follows (48,49).

$$\frac{t}{qt} = \frac{1}{K_2 q_e^2} + \frac{1}{q_e} t \tag{15}$$

where q_e and q_t are the amount of Ru adsorbed at equilibrium and at time t respectively and K_2 is the rate constant for pseudo-second-order sorption.

A pseudo-second-order plot of t/q_t versus t for sorption of Ru on the NiS–PMMA composite material is shown in Fig. 12. The kinetic constants are given in Table 5.

(iii) *Second-order model*
The Langergren second order equation is given by (46,47):

$$\frac{1}{q_e - q_t} = \frac{1}{q_e} + Kt \tag{16}$$

where q_e and q_t are the amount of Ru sorbed at equilibrium and at time t respectively and K is the rate constant for second order sorption.

Figure 13 shows a second-order plot of $(1/(q_e\text{-}q_t)$ versus t for sorption of Ru on NiS–PMMA composite material. The kinetic constants are given in Table 5.

A comparison of Figs. 11–13 and the kinetic data listed in Table 5 showed that the pseudo-second-order has provided the best fit. Therefore, the Langergren pseudo-second-order kinetic model is applicable for sorption of Ru on the NiS–PMMA composite materials.

Sorption Mechanism

Adsorption is a phenomenon which describes the way by which a molecule of an adsorbate forms a bond to the surface of an adsorbent. Adsorption is classified as physical adsorption and chemisorption depending on bond energies or enthalpy.

The sorption data obtained with Freundlich, Langmuir, and D–R isotherms indicates physical sorption and the value of E, the mean sorption energy obtained is $8.153\,kJ \cdot mole^{-1}$, $6.651\,kJ \cdot mole^{-1}$, and $7.892\,kJ \cdot mole^{-1}$ for NiS–PMMA(C), NiS–PMMA(G), and NiS–PMMA(E) composite material. The sorption data follow Freundlich

TABLE 5
Kinetic constants

	First order		Pseudo second order		Second order	
Composite material	K_L	R^2	K_2	R^2	K	R^2
NiS–PMMA(C)	0.1313	0.9887	10.73	0.9999	34.17	0.949
NiS–PMMA(G)	0.0598	0.93	22.103	0.99999	6.596	0.993
NiS–PMMA(E)	0.05711	0.935	18.25	0.99998	4.908	0.990

and D–R isotherm, but linearity was not observed in the Langmuir sorption isotherm. These observations reflect multilayer sorption. The negative value of ΔG indicates the spontaneous nature of the sorption. The low value of mean sorption energy is not favoring the ion exchange type of interaction suggesting the interaction between the ruthenium species in alkaline solution with NiS–PMMA composite material must be of ion dipole type.

To have a scientific approach for adsorption behavior of ^{106}Ru on both the NiS–PMMA composite material, the use of a suitable adsorption model was necessary. One such model used by Zhang et al. (50) was used to study the adsorption behavior of ^{106}Ru.

If one assumed that the adsorption process of ^{106}Ru on NiS–PMMA was monolayer, then the adsorption rate of ^{106}Ru on the adsorbent was mainly affected by the available concentration of ^{106}Ru and the effect of time on the adsorption was not significant. The adsorption equation was expressed as

$$\frac{dC_t}{dt} = K(C_o - C_t) \tag{17}$$

where C_o and C_t is the adsorbed amount of ruthenium at equilibrium and at time t respectively and K is the adsorption constant for monolayer adsorption.

On integration, the equation can be written as,

$$-\ln\,(1 - F) = K_s\,t \tag{18}$$

where $F = C_t/C_o$.

The plot of $-\ln(1 - F)$ versus time t should be a straight line and the slope of the resultant line corresponds to K_s.

The adsorption behavior of ruthenium on NiS–PMMA composite material was investigated with above Eq. (18). The results are shown in Fig. 14. As seen from the figure, the graph obtained is not linear, thus the adsorption may not be monolayer. This is in agreement that the adsorption does not follow the Langmuir isotherm.

If one assumed that the adsorption of ruthenium on the adsorbent was multilayer, then the adsorption rate increased with an increase in the available concentration while it decreased with contact time. The adsorption rate equation was then given by,

$$\frac{dC_t}{dt} = K_m \frac{(C_o - C_t)}{t} \tag{19}$$

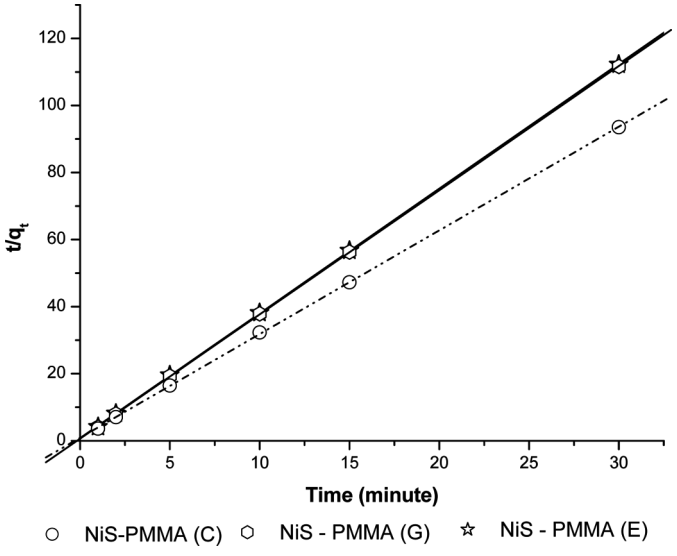

FIG. 12. Pseudo second order plot for sorption of Ru on NiS–PMMA composite material.

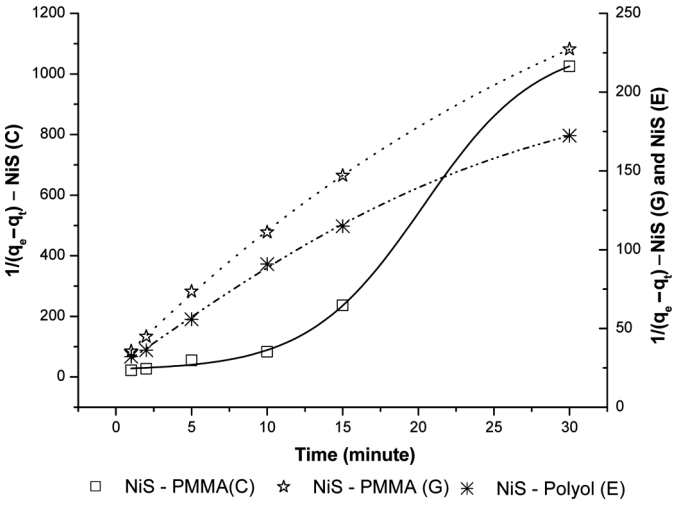

FIG. 13. Second order plot for Ru sorption on NiS–PMMA composite material.

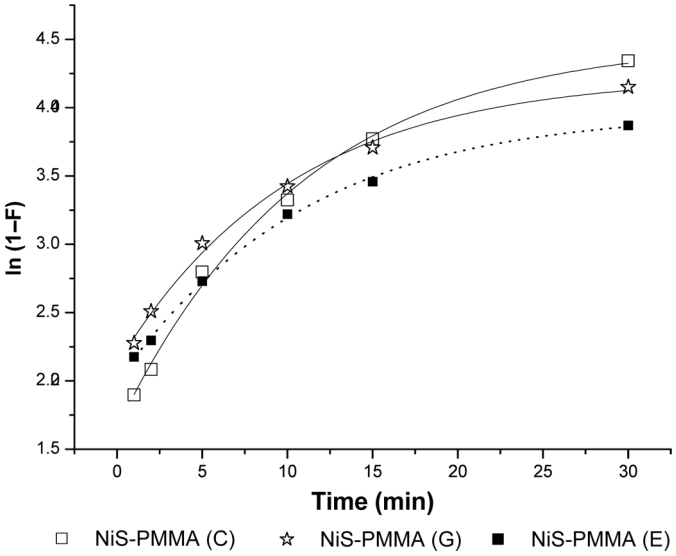

FIG. 14. Relatiionship between –ln(1 – F) and t.

above equation can on integration can be written as,

$$-\ln(1-F) = K_m \ln t \qquad (20)$$

where K_m is the adsorption constant for multilayer adsorption.

The plot of –ln(1 – F) versus ln t should be a straight line and the slope of the resultant line corresponds to K_m.

The adsorption behavior of ruthenium on NiS–PMMA composite material was investigated with the above Eq. (20). The results are shown in Fig. 15. As seen from the figure, the graph obtained is linear; thus the adsorption is multilayer. This is in agreement that the adsorption follow the Freundlich isotherm.

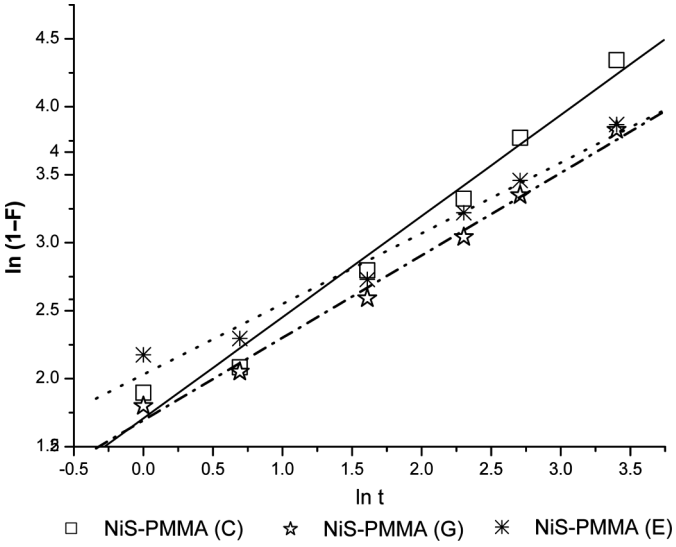

FIG. 15. Relationship between –ln(1 – F) and ln t.

CONCLUSIONS

The NiS–PMMA composite material prepared in this study has good K_d value for ^{106}Ru removal. All the three composite material are working satisfactorily in alkaline condition. The effect of salt concentration on K_d value is negligible. 20–30% of NiS loading on PMMA material is suitable for the effective removal of ^{106}Ru from alkaline radioactive liquid waste. The sorption of ^{106}Ru on the composite material is observed to follow Freundlich and D-R isotherms. The value of the sorption energy E on the basis of experimental data of various sorption isotherms indicates a multilayer sorption. This is further confirmed by applicability of the Zhang model. The sorption process is spontaneous and endothermic in nature. Based on these findings, it is concluded that the NiS–PMMA composite material can be used for the effective removal of ^{106}Ru. From the kinetic studies, it can be concluded that the sorption of Ru from solution on NiS–PMMA composite material surface is due to intraparticle diffusion and it is following the pseudo-second-order pattern, which is an indication of multilayer sorption.

ACKNOWLEDGEMENTS

The authors are thankful to Shri R. D. Changrani, Chief Superintendent, NRGF (T) for his guidance and interest in the work and also to Shri Kanwar Raj, Head, Waste Management Division, BARC, Mumbai for his consistent encouragement with the work.

REFERENCES

1. Ramanujam, A. (1999) Partitioning of actinides from high level waste of PUREX origin using octylphenyl-N-N′-diisobutylcarbomoylmethyl phosphine oxide (CMPO) based supported liquid membrane. *Separation Science and Technology*, 34: 1717–1728.
2. Ansari, S.A.; Pathak, P.N.; Manchanda, V.K.; et al. (2004) N,N,N′,N′ Tetra Octyl Digllycolamide (TODGA): A promising extractant for actinide – partitioning from high level waste. *SESTEC*-2004: 166–167.
3. International Atomic Energy Agency. (1985) Chemical durability and related properties of solidified high level waste forms. Technical Reports Series no. 257, IAEA,Vienna.
4. Yeotikar, R.G.; Sonavane, M.S.; Shah, J.G.; Kanwar, R. (1993) Development of vitrified matrix for high level waste and its characterisation – experience at WIP, Tarapur. National symposium on management of radioactive and toxic waste (SMART-93) Kalpakkam, 257–260.
5. Yeotikar, R.G.; Kaushik, C.P.; Johnson, G.; Kanwar, R. (1995) Treatment of alkaline intermediate level radioactive waste. NUCAR 95 – IGCAR, Kalpakkam, Feb. 21–24, 429–430.
6. Mercer, E.E.; Campbell, W.M.; Wallace, R.M. (1964) Chloro complexes of nitrosylruthenium. *Inorganic Chemistry*, 3 (5): 1018–1024.
7. Scargill, D.; Lyon, C.E.; Large, N.R.; Fletcher, J.M. (1965) Nitroaquo complexex of nitrosylruthenium III. *Journal of Inorganic Nuclear Chemistry*, 27: 161–171.
8. Bottomley, F. (1978) Nitrosyl complexes of ruthenium. *Co-ordination Chemistry Review*, 26 (1): 7–32.
9. Rudstam, G. (1959) Studies on nitroslruthenium complexes in nitric acid using repeated extractions. *Acta Chemica Scandinavica*, 13: 1481–1501.

10. Siczek, A.A.; Steindler, M.J. (1978) The chemistry of ruthenium and zirconium in the PUREX solvent extraction process. *Atomic Energy Review*, 16 (4): 575–618.
11. El-Absy, M.A.; El-Amir, M.A.; Mostafa, M.; Abdel Fattah, A.A.; Aly, H.M. (2005) Separation of fission products ^{106}Ru and ^{137}Cs from aged uranium targets by sequential distillation and precipitation in nitrate media. *Journal of Radioanalytical and Nuclear Chemistry*, 266 (2): 295–305.
12. Cotton, F.; Wilkinson, G. (1972) *Advance Inorganic Chemistry*, 3rd Ed.; John Wiley & Sons Inc.: NY, 1012.
13. Berak, L.; Uher, E.; Marhol, M. (1975) Sorbents for the purification of low and medium level radioactive waters. *Atomic Energy Review*, 13: 325–367.
14. Gandon, R.; Boust, D.; Bedue, O. (1993) Ruthenium complexes originating from the purex process: Coprecipitation with copper ferrocyanides via ruthenocyanide formation. *Radiocheim Acta*, 61: 41–45.
15. Jain, S.; Pawaskar, C.S.; Johnson, G.; Budhwar, R.K.; Kumar, S. (2006) Removal of ^{106}Ru and ^{125}Sb from radioactive liquid waste. SESTEC – 2006, Mumbai, 278–279.
16. Samanta, S.K.; Theyyunni, T.K. (1994) Removal of radioruthenim from alkaline intermediate level radioactive waste solution: A laboratory investigation. BARC/1994/E/012.
17. "Inorganic Ion Exchangers and Adsorbents for Chemical Processing in the Nuclear Fuel Cycle" IAEA – TECDOC – 337, 1984 – "Radioactive ruthenium removal from liquid wastes of M0^{99} production process using zinc and charcoal mixture." 63–74.
18. Samanta, S.K. (1992) Studies on the removal of ruthenium from radioactive waste. Nuclear and Radiochemistry Sumposium, Andhra University, Vishakhapatanam, Dec. 21–24, 1992.
19. Syed, A.A.; Dinesan, M. (1992) Polyaniline: A conducting polymer as a novel anion – exchange resin. *Analyst*, 117: 61–66.
20. Syed, A.A.; Dinesan, M. (1991) Polyaniline: A novel material – review. *Talenta*, 38: 815–837.
21. Balarama Krishna, M.V.; Arunachalam, J.; Prabhu, D.R.; Manchanda, V.K.; Kumar, S. (2005) Removal of Ru^{106} from actual low – level radioactive waste solutions using polyaniline as anion – exchanger. *Separation Science and Technology*, 40: 1313–1332.
22. Czerwinski, A.; Voulgaropoulos, A.; Mark, H.B. (1989) A radiotracer method for the study of ruthenium adsorption on polysulfur nitride. *Journal of Radioanalytical Nuclear Chemistry, Letters*, 85 (3): 173–180.
23. Motojima, K. (1989) Removalof ruthenium from PUREX process – extraction of ruthenium tetroxide with paraffin oil and filtration of ruthenium dioxide. *Journal of Nuclear Science and Technology*, 26 (3): 358–364.
24. Motojima, K. (1990) Removalof ruthenium from PUREX process – fundamental research of electrolytic oxidation of ruthenium. *Journal of Nuclear Science and Technology*, 27 (3): 262–266.
25. Singh, U.S.; Sonar, N.L.; Kore, S.G.; Mishra, P.K.; Sonavane, M.S. (2005) Development of method for treatment of Ru^{106} rich radioactive liquid waste with high salt content. NUCAR 2005, Gurunanak Dev University, Amritsar, March 15–18, 371–372.
26. Sonar, N.L.; Mishra, P.K.; Kore, S.G.; Sonavane, M.S.; Kulkarni, Y.; Kanwar, R.; Manchanda, V.K. (2009) Treatment of ^{106}Ru present in intermediate level radioactive liquid waste with nickel sulphide. *Separation science and Technology*, 44: 506–515.
27. Sonar, N.L.; Sonavane, M.S.; Valsala, T.P.; Kulkarni, Y.; Kanwar, R.; Manchanda, V.K. (2008) Use of nickel sulphide – PMMA composite beads for removal of ^{106}Ru from alkaline radioactive liquid waste. SESTEC – 2008, DAE-BRNS Symposium. Delhi, 365–366.
28. Feldmann, C.; Metzmacher, C. (2001) Polyol mediated synthesis of nanoscale MS particles (M=Zn,Cd,Hg). *Journal of Material Chemists*, 11: 2603.
29. Guozhen, Shen; Di, Chen; Kaibin, Tang; Xianming, Liu; Liying, Huang; Yitai, Qian. (2003) General synthesis of metal sulfides nanocrystalines via a simple polyol route. *Journal of Solid State Chemistry*, 173: 232–235.
30. Gabriel, J.; Shah, J.G.; Valsala, T.P. (2003) Spherical AMP composite ion exchange material for treatment of acidic intermediate level waste. Nuclear and Radiochemistry Symposium - NUCAR-2003, 567–568.
31. Karanjai, M.K.; Dasgupta, D. (1987) Preparation and study of sulphide thin films deposited by the dip technique. *Thin Solid Films*, 155: 309.
32. Tohge, N.; Asuka, M.; Minami, T. (1992) Sol – gel preparation and optical properties of silica glasses containing Cd and Zn chalcogenide microcrystals. *Journal of Non-Crystalline Solids*, 147–148: 652.
33. Kitsev, G.E.; Sokolva, T.P. (1970) Chemical deposition of thin zinc selenide films. *Russian Journal of Inorganic Chemistry*, 15: 167–169.
34. Metilda, P.; Sanghmitra, K.; Mary Gladis, J.; Naidu, G.R.K.; Prasada Rao, T. (2005) Amberlite XAD-4 functionalized with succinic acid for the solid phase extractive preconcentration and separation of uranium (VI). *Talanta*, 65: 192–200.
35. Dubinin, M.M.; Raushkevich, I.V. (1947) *Proc. Acad. Sci. USSR Phys. Chem. Sect.*, 55: 331.
36. Polanyi, M. (1932) Adsorption of gases by solids. *Trans. Faraday Society*, 28: 316–320.
37. Ahmad, H.; Afzal, M.; Saleem, M.; Hasany, S.M. (1994) Adsorption of radiocobalt on lead oxide from aqueous solution. *J. Radioanalytical and Nuclear Chemistry*, 181 (1): 117–129.
38. Horsfall Jnr, M.; Spiff, A.I. (2005) Effects of temperature on the sorption of Pb^{2+} and Cd^{2+} from aqueous solution by caladium bicolor (Wild Cocoyam) biomass. *E – Journal of Biotechnology*, 8(2).
39. Qadeer, R.; Hanif, J.; Saleem, M.; Afzal, M. (1993) Surface characterisation and thermodynamics for adsorption of Sr^{2+}, Ce^{3+}, Sm^{3+}, Gd^{3+}, Th^{4+}, UO_2^{2+} on activated charcoal from aqueous solution. *Colloid and Polymer Science*, 271: 83–90.
40. Guidal, E.; McCarrick, P.; Tobin, J.M. (2003) *Separation Science and Technology*, 38 (12–13): 3049.
41. Weber, W.J.; Morris, J.C.; Sanit, J. (1963) Kinetics of adsorption on carbon from solutions. *American Society Civil Engg.*, 89: 31–60.
42. Kannan, N.; Sundaram, M.M. (2001) Kinetics and mechanism of removal of methylene blue by adsorption on various carbons—a comparative study. *Dyes Pigments*, 51 (1): 25–40.
43. Malik, P.K. (2003) Use of activated carbons prepared from sawdust and rice-husk for adsorption of acid dyes: A case study of acid yellow 36. *Dyes Pigments*, 56 (3): 239–249.
44. Poots, V.J.P.; Mckay, G.; Healy, J.J. (1978) Removal of basic dye from. effluent using wood as an adsorbent. *J. Water Pollution Control Federation*, 50: 926–935.
45. Chiarizia, R.; Horwitz, E.P.; Alexandratos, S.D. (1994) Uptake of metal ions by a new chelating IX resin, Part-IV: Kinetics. *Solvent Extraction and Ion Exchange*, 12: 211–237.
46. Langergren, S. (1898) Zur Theorie der sogenannten adsorption gelostn. Stoffe. Stcok. *Ak Handl. Bihay*, 24 (Afd. 1): 39.
47. An Ong, Soon; Seng, Chye – Eng; Lim, Poh-Eng. (2007) Kinetics of adsorption of Cu(II) and Cd(II) from aqueous solution on rice husk and modified rice husk. *E – Journal of Environmental, Agricultural and Food Chemistry*, 6 (20): 1764–1774.
48. Ho, Y.S.; Mcay, G.; Waste, D.A.J.; Forster, C.F. (2000) Study of the sorption of divalent metal ions on to peat. *Adsorption Science and Technology*, 18: 639–650.
49. Ho, Y.S.; Mcay, G. (1999) Pseudo – second order model for sorption processes. *Process Biochemistry*, 34: 451–465.
50. Zhang, A.; Wei, Y.; Kumagai, M. (2004) Synthesis of a novel macroporous silica-based polymeric material containing 4,4′,(5′)-di(tert-butylcyclohexoano)-18-crown-6 functional group and its adsorption mechanism for strontium. *Reactive & Functional Polymers*, 61: 191–202.